View metadata, citation and similar papers at core.ac.uk
brought to you by CORE
provided by KITopen

OXIDATION AND QUENCH BEHAVIOR OF COLD SPRAYING CR COATED ZIRCALOY FUEL CLADDING UNDER SEVERE ACCIDENT SCENARIOS

Chongchong Tang[*], *Mirco Grosse*, *Martin Steinbrueck*

Institute for Applied Materials (IAM), Karlsruhe Institute of Technology (KIT), D-76021 Karlsruhe, Germany
Chongchong.tang@kit.edu

Koroush Shirvan

Department of Nuclear Science and Engineering, Massachusetts Institute of Technology, 77, Massachusetts Avenue, Cambridge, MA 02139, USA

The oxidation performance and quench behavior of cold spraying Cr coated Zircaloy-4 cladding tubes were investigated from 1100°C up to 1500°C in steam. The coated samples displayed significantly improved oxidation resistance, good thermal shock resistance and high post-quench ductility during oxidation at 1100°C and 1200°C for 1 hour accompanied by subsequent quench in water. However, substantial bending of the coated tubes was observed during oxidation at 1100°C, which led to loss of protective effect of the coatings on the tensile (convex) side. The underlying mechanisms for the occurrence of bending phenomenon at such temperature seems to be related with the residual stress state and high-temperature creep behavior of the coated cladding. Once the oxidation temperature exceeds the Cr-Zr eutectic temperature (~1330°C), oxygen drives the Cr diffusing inwardly (owing to the low solubility of Cr in ZrO_2) and the formation of liquid phase contributes to rapid degradation of the coated cladding, connected with a much faster oxidation rate compared to the uncoated reference sample.

I. INTRODUCTION

The attractive properties of zirconium alloys, for instance small neutron capture cross section, good corrosion behavior and irradiation performance, make them an ideal choice for application of nuclear fuel cladding and structural components during normal operations. However, during accident scenarios, the rapid exothermic oxidation reaction between zirconium and steam can generate a large amount of heat and hydrogen, threatening the reactor safety and may leading to serious reactor damage [1]. The Fukushima-Daiichi accidents in 2011 highlighted the demand to explore and develop advanced accident tolerant fuel (ATF) claddings that provide enhanced safety margins under accident scenarios of water-cooled nuclear reactors. One near-term strategy can be surface modification of state-of-the-art zirconium-based alloy cladding with innovative metallic or ceramic coatings [2,3]. This solution is an incremental change to the currently standardized UO_2 fuel/Zr alloy cladding structures but allows for a more rapid licensing pathway.

Among the variety of coating materials being investigated, the pure metallic Cr coating represents one of the most attractive and promising options for near-term implementation. Cr coatings, deposited by either cold spray or physical vapor deposition (PVD), features good adhesion strength and irradiation resistance [4–7]. Formation of a superficial Cr_2O_3 layer in oxidizing environments renders the coated cladding an extremely low corrosion rate under simulated normal operational conditions and significantly improved high-temperature steam oxidation resistance with reduced cladding creep and ballooning during LOCA conditions. The original objective of the enhanced ATF materials is to offer additional coping time in case of severe accident scenarios. However, only a few works are devoted to evaluation and qualification of oxidation and quench performances of Cr coated cladding under simulated severe accident scenarios [8,9]. In this paper, the oxidation performance and quench behavior of cold spraying Cr coated Zircaloy-4 tubes were investigated from 1100°C up to 1500°C in steam using the single-rod quench facility QUENCH-SR. The distinct failure behaviors, depending on the oxidation temperatures, of cold spray Cr coated cladding tubes will be presented and discussed.

II. EXPERIMENT

II.A. Samples

Chromium coated (deposited by cold spray process) Zircaloy-4 cladding tube samples together with uncoated ones as reference were tested in this study. The coating was applied by Plasma Processes with process parameters noted in reference [10]. The tubes were filled with zirconia pellet inside and the ends were welded.

These tubes have an outer diameter of 9.7 mm and a length of 130 mm. The cladding thickness is ~0.57 mm with a ~20-70 µm thick Cr coating layer for coated samples. However, the outer surfaces were not completely covered by the coatings. At one end side ~20 mm length was not coated, as shown in Fig. 1. To measure and control the temperature during experiments, three thermocouples were attached to the sample surface via a Platinum-Rhodium wire. The lower thermocouple (TC_l) was mounted 20 mm from the bottom of the tube (coated side), the middle thermocouple (TC_m) was mounted 50 mm from the bottom and the upper thermocouple (TC_u) was mounted 105 mm from the bottom near the border between the coated and uncoated region (Fig. 1). A two-color pyrometer was also installed to monitor the temperature at a position close to TC_m. The thermocouple TC_m, positioned in the center of the heated zone, was selected as an input signal to control the temperature during experiments.

Fig. 1. Appearance and locations of thermocouples of cold spraying Cr coated Zircaloy-4 cladding tube before testing.

II.B. Oxidation and quench tests

Two kinds of tests have been performed, i.e. isothermal test and transient test, using the single rod quench facility (QUENCH-SR) of KIT. The samples were positioned vertically inside a quartz tube with the upper side (uncoated end) fixed. Induction coils heated the samples using a 20 kW oscillator, at a frequency of up to 700 kHz. A valve of a cylinder filling with water beneath allows quenching the sample by water via mechanically driving the cylinder upwards. The furnace was connected to a Balzers GAM 300 quadrupole mass spectrometer (MS) for quantitative analysis of the gaseous reaction products.

In the isothermal tests, the samples were heated to pre-defined temperatures (1100°C, 1200°C or 1300°C) with 10 K/min in argon. Once the temperature was reached, steam was introduced into the furnace at a flow rate of 60 g/h. The samples were isothermally oxidized for 1 hour. Temperature gradient existed along the axial direction of the tube owing to non-uniform heating. After exposure, the samples were quenched in water if possible (bending or melting of tubes occurred sometimes did not allow finally quenching, see results below). During the transient tests, the steam was injected into the furnace at 800°C, then the sample was heated up to 1500°C in steam without quenching. One isothermal test at 1200°C and one transient test of uncoated reference tubes were also conducted to compare their behaviors. After testing, the samples were characterized using various methods, such as optical and electron microscopy.

III. RESULTS

III.A. Isothermal tests

III.A.1. Isothermal test at 1100°C

The first isothermal test was performed at 1100°C; the temperature profiles, hydrogen and steam flow rates during the test are presented in Fig. 2. Fig. 3 shows the post-test appearances of the samples. As seen in Fig. 2, the temperature recorded by the TC_m was stabilized at 1100°C during the isothermal exposure. The temperature measured by the pyrometer was around 100°C higher, accompanied by a slight gradual decrease. The temperatures at the lower and upper regions of the tubes recorded by other two thermal couples were around 1010°C and 880°C, respectively. Similar slightly decreasing temperatures were observed during the exposure, likely due to the cooling effect by the argon and steam flow. A high peak of hydrogen release was observed once the steam was introduced, indicating initially fast oxidation of the fresh surface. The hydrogen release rate then decreased continuously, except small bumps (likely owing to cracking of the coatings) on the curve marked by the arrows.

Substantial bending of the coated tube occurred during the test (Fig. 3), prohibiting final quenching of the tube because of potential damage to the facility. Thus, the sample was cooled in argon atmosphere inside the reaction tube without quenching. The surface color of the sample transformed from metallic luster to green owing to the growth of an oxide layer. A small section of the attachment wire at the middle region was incorporated into the tube surface, which could not be easily separated as seen in Fig. 3. Cracking of the coatings near and beneath the wire was shown. The maximum displacement of the tube (at the coated end) reached approximately 10.24 mm, larger than the diameter of the tube.

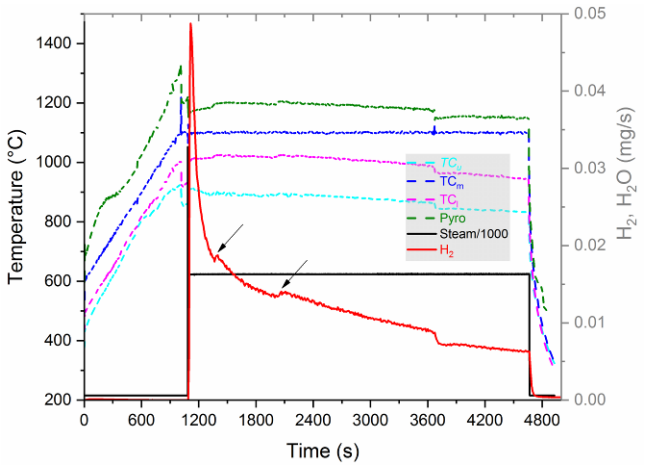

Fig. 2. Temperature profiles, hydrogen and steam flow rates during the isothermal test at 1100°C for 1 h.

Fig. 3. Post-test appearance of the sample after the first isothermal test at 1100°C showing significant bending.

Fig. 4 displays the degree of bending as a function of time in the initial stage of oxidation. The first sign indicating the occurrence of bending was before starting the steam injection. However, the degree of the bending was very small compared to the bending occurring later with steam flow. Additionally, the majority of the bending took place within the first 5 minutes of steam oxidation.

Fig. 5 are optical images of cross section of the samples at ~55 mm (distance from the coated end, similarly hereinafter). At the tensile side, nearly all coatings have peeled off from the sample surface at the location of maximum tensile strain. Significant oxidation and consumption of the metallic matrix at this region resulted in formation of a thick ZrO_2 layer with loss of strength and ductility, Fig. 5 (a), causing fracture of the tube during post-test examination. Some discontinuous fragments of the Cr coating attached at adjacent areas as shown in the inserted image. The thickness of the ZrO_2 layer decreased gradually as the position changed from the tensile side (convex) to the compression (concave) side. In the compression side, the coatings revealed good oxidation resistance and high adherence, without cracking or delamination (Fig. 5 (b)). A thin oxide layer formed on the surface and no evidence shows oxidation of the substrate. The typical high roughness of the coatings deposited by cold spray process was also clearly seen.

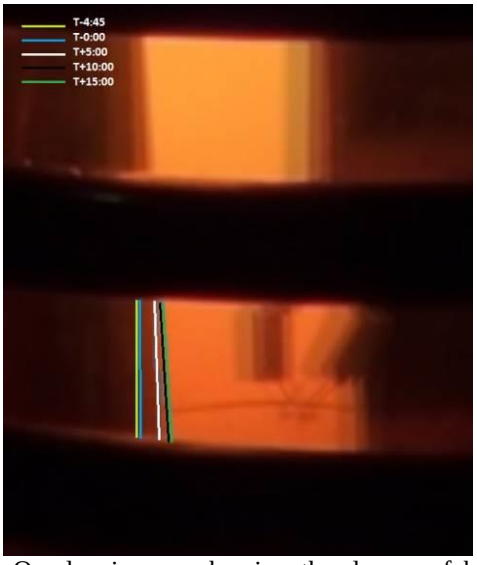

Fig. 4. Overlay images showing the degree of bending during test. T-0:00 represent the moment when steam was introduced into the furnace.

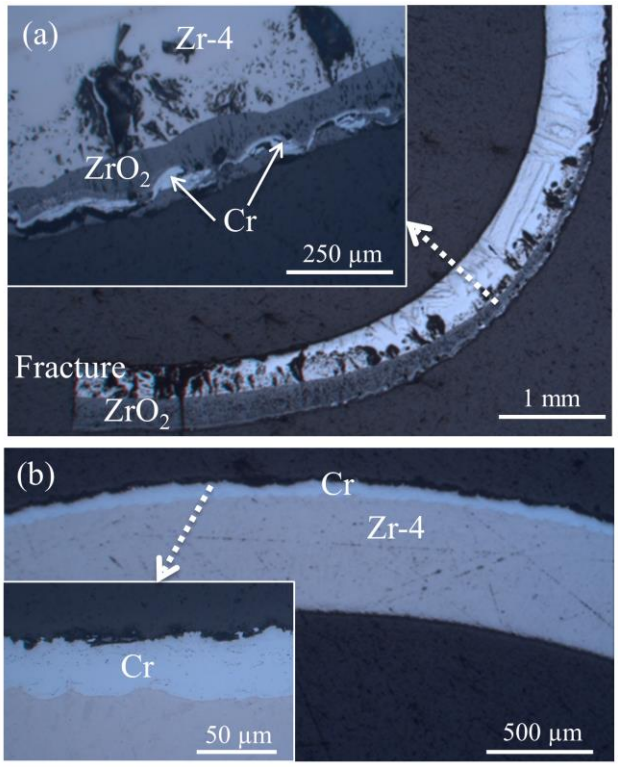

Fig. 5. Optical images of cross section of the samples at elevation ~55 mm, (a) tensile side and (b) compression side of the bending tube.

The test has been repeated and in order to avoid the bending and finally quench the tube, steam was introduced earlier during the heating phase at 800°C allowing growth of a protective chromium oxide layer.

However, during the second test the sample started to bend again, as seen in Fig. 6. Thus, this sample was not quenched again. During the exposure, the tensile side of the tube appeared brighter and hotter than the compression side. The final maximum displacement of the tube was similar to the first one. Note that bending of the tube probably represents a universal deformation mode at such temperature. No uncoated reference test was performed at this temperature due to the limited number of samples. However, our previous investigations on steam oxidation and quench of bare Zr alloy cladding tubes under similar conditions at 1100°C did not show bending phenomenon of the tube [11].

Fig. 6. Appearances of the sample during the second test at 1100°C (upper) and after the test (bottom).

Fig. 7 compares the hydrogen release behaviors during the two tests. Pre-oxidation of the samples owing to early introduction of steam reduced the initial high release rate of hydrogen when the temperature was reached. The intensity of the initial peak was much lower than that of the second test. The total hydrogen productions were comparable, slightly less for the second test likely due to introduction of steam at lower temperature. The oxidation kinetics for both tests, as proved by the hydrogen production curves, roughly followed a parabolic law.

III.A.2. Isothermal test at 1200°C

The isothermal oxidation test at 1200°C was successful (no obvious bending of the tube) with final quenching of the tube in water. The temperature profiles, hydrogen and steam flow rates during the test were shown in Fig. 8. Similar to the tests at 1100°C, the temperature recorded by the pyrometer was about 210°C to 100°C higher than that of TC_m. In the quench phase, the temperature of the tube dropped from 1200°C to 60°C in ~ 5 s. The hydrogen curve also demonstrated similar evolution trend as at 1100°C, but without bumps on the curve.

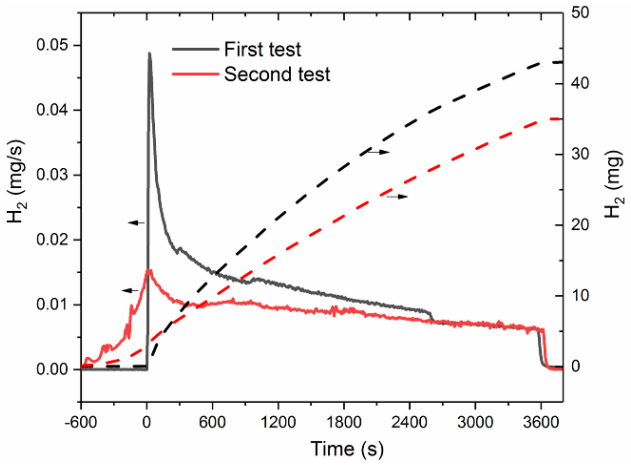

Fig. 7. Comparison of the hydrogen release rate and total hydrogen production during the two isothermal tests at 1100°C.

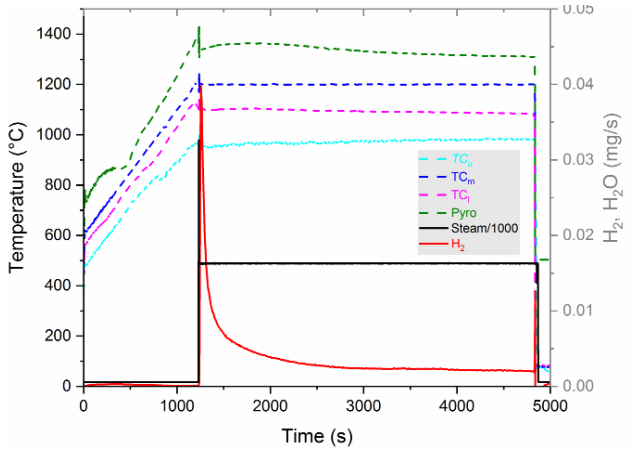

Fig. 8. Temperature profiles, hydrogen and steam flow rates during the isothermal test at 1200°C for 1 h.

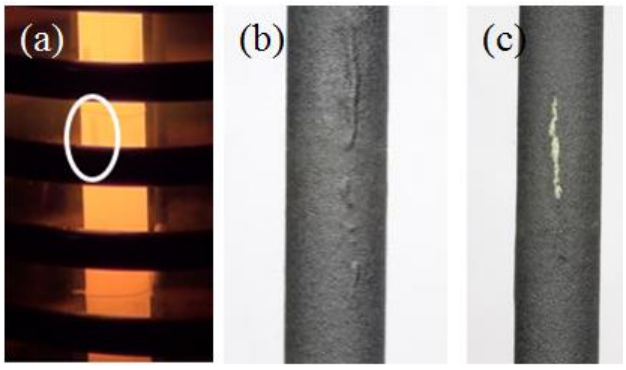

Fig. 9. Appearances of the sample (a) during the test, (b) and (c) after the test at 1200°C.

Fig. 9 displays the appearance of the sample during and after the test. Interestingly, few dark stripes were observed on the sample surface during the isothermal exposure period, one highlighted in Fig. 9 (a). Via

examining the post-test appearance it turned out that these stripes are indications of delamination within the coating layer and after quenching some oxide layer was spalled off, as seen in Fig. 9 (b) and (c). In addition, no bending of the tube appeared. The Cr coating layer revealed excellent thermal shock resistance and adherence, without cracking and spallation except at those dark stripes.

Fig. 10 shows the cross section and surface structure of the samples after testing. Delamination was observed at two interfaces, i.e. Cr_2O_3 scale/Cr coating interface and Cr coating/Zr alloy substrate interface. No sign shows oxidation of the substrate or the Cr coating inside the voids generated by delamination. Spallation of the oxide scale and cracking of the Cr coating layer at these delamination areas were seen during cooling and post-test examination.

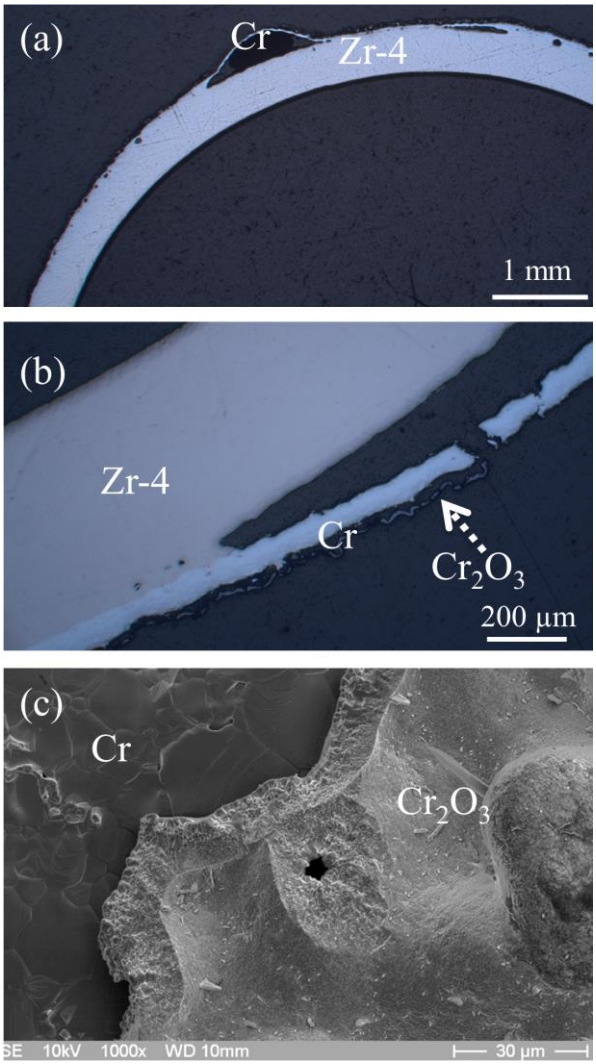

Fig. 10. (a) and (b) optical images of cross section located ~ 55 mm, (c) SEM image of surface of the samples after testing at 1200°C.

A reference uncoated Zircaloy-4 tube was tested at 1200°C for 1 hour and Fig. 11 compares the hydrogen production of the two tests together with the first test at 1100°C. The total hydrogen production was 186.2 mg for the uncoated sample oxidized at 1200°C. In case of the coated sample, it was 13.4 mg, ~14 times less relative to uncoated one. As seen in of the inserted image of Fig. 11, the uncoated tube fractured into few pieces during quench owing to oxidation converting Zry metal to brittle oxide of the cladding tube, while the coated one still remained its physical integrity (Fig. 9). This indicates that the Cr coating layer can remarkably reduce the oxidation kinetics of the cladding with simultaneously significant less hydrogen production and higher post-quench ductility at such temperature. The hydrogen production at 1100°C was even much higher (43.3 mg) than that at 1200°C because bending of the tube led to cracking and spallation of the coating layer.

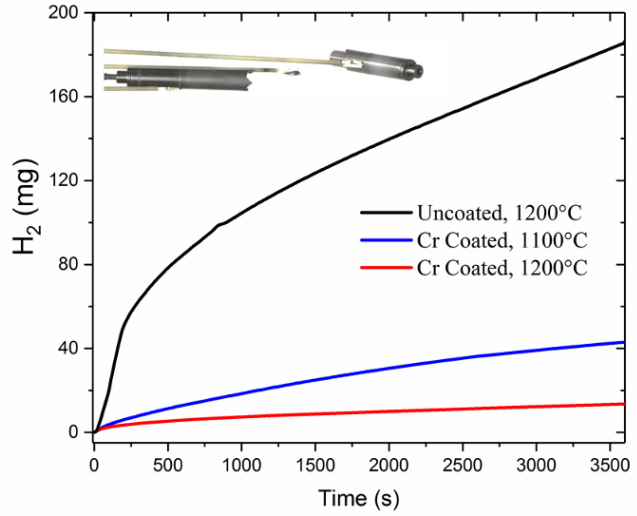

Fig. 11. Comparison of the hydrogen production of three tests. Inserted image shows fracture of uncoated Zircaloy-4 tube after 1200°C oxidation and quench.

III.A.3. Isothermal test at 1300°C

The original plan of the isothermal test at 1300°C, like before, was oxidizing of the sample for one hour in steam followed by quenching. Fig. 12 shows the temperature and gas flow and Fig. 13 illustrates the appearances of the sample of this test. However, during the heating period at a temperature around 1215°C the platinum-rhodium wire fixing the TC_m disappeared (Fig. 13). After this moment the temperature started to fluctuate heavily, as shown in Fig. 12. This is logical since the temperature was controlled via TC_m. A few moments later TC_m detached from the sample, and the temperature on the other thermocouples increased very fast, TC_u went from 944.5°C to 1130.7°C in 17 s. At this point, it was

noticed that the sample started to melt and the test was terminated. The steam flow, i.e. the oxidation period, lasted about 70 s. A very high peak of hydrogen was recorded as displayed in Fig. 12. The reason for the disappearing of the wire was not clear yet, probably because of a melt formation. The eutectic reaction temperature between Pt and Cr is at 1514°C, between Cr and Zr is at 1332°C, and between Pt and Zr is at 1187°C [12]. The eutectic reaction temperature of the Pt-Cr-Zr ternary system clearly is below 1187°C. Even though no direct contact of the wire with the Zircaloy-4 substrate took place, the high roughness of the Cr coating layer may have resulted in the formation of ternary liquid phases at temperatures below 1300°C owing to interdiffusion between the Cr coating layer and the substrate, especially at locations where the coating layer had lower thickness.

Even though the test failed, it proved that the protective capability of the Cr coating was highly challenged once the temperature exceeded the Cr-Zr eutectic temperature. Formation of liquid phase accompanied by its continuous displacement and movement exposed the inside zirconia pellets at some places and resulted in rapid degradation of the whole cladding tube, Fig. 13.

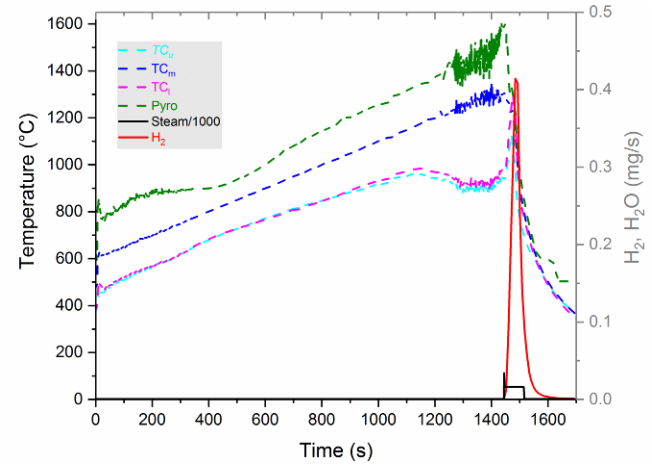

Fig. 12. Temperature profiles, hydrogen and steam flow rates during the isothermal test at 1300°C.

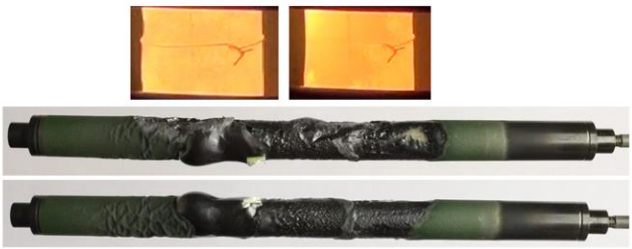

Fig. 13. Appearances of the samples during the test (upper) and after the test (bottom) at 1300°C.

III.B. Transient tests

Fig. 14 shows the temperature profile and hydrogen release rates of coated and uncoated samples during the transient test from 800°C to 1500°C in steam. The hydrogen release rate increased virtually linear with rising of oxidation temperature for the uncoated tube. In case of the Cr coated sample, the hydrogen rate first increased slowly, several times lower than that of uncoated one. The hydrogen release rate then accelerated at temperature around 1250°C, indicating fast oxidation rate of Cr at elevated temperatures and/or loss of the protective effect of the Cr scale. A steeply increased hydrogen release rate was observed at temperatures above approx. 1410°C. And immediately, the hydrogen release rate surpassed that of the uncoated reference Zircaloy-4 at temperature above ~1450°C, generating a significantly higher hydrogen peak which was not observed for the uncoated sample. This phenomenon should attribute to formation of liquid phases once the temperature exceeded the Cr-Zr eutectic temperature (~1330°C) leading to the failure of the coatings and rapid oxidation of the underneath substrate. According to the Ellingham diagram, oxygen has a higher affinity to zirconium than to chromium. When the zirconium in the eutectic melt reaches the chromia layer, the inner part of the chromia layer can be reduced. The total hydrogen productions were 125.3 mg and 81.5 mg for the uncoated and coated samples, respectively.

Fig. 15 are post-test appearances of the coated and uncoated samples after the transient test. The coated tube preserved its integrity without fracture. In comparison, the uncoated tube has cracked and fracture after the test. Examination of the coated sample surfaces clearly showed the formation of protrusions at the hottest region (middle) and the surface became rougher. No large liquid drops, as seen in Fig. 13, were observed here.

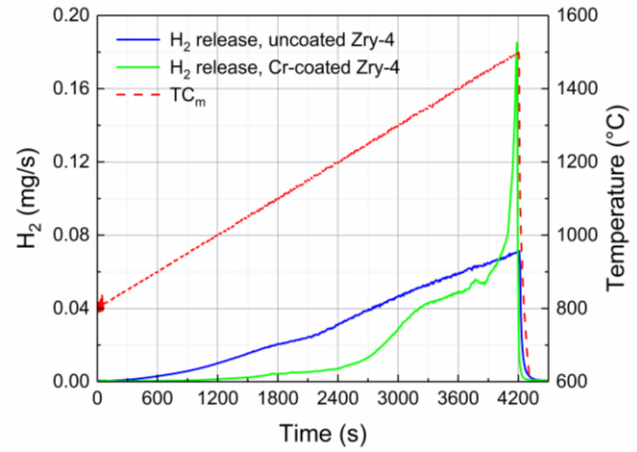

Fig. 14. Temperature profile and hydrogen flow rates of the transient tests from 800°C to 1500°C in steam.

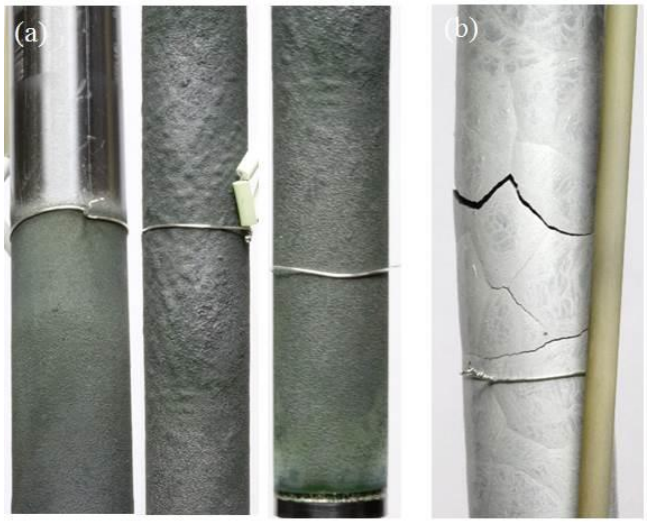

Fig. 15. Post-test appearances of the (a) coated and (b) uncoated samples after the transient test.

The surface and cross section microstructures of the Cr coated tube after the transient test are shown in Fig. 16. EDS analysis confirmed that the surface was covered by Cr_2O_3. Mirco-cracking of the oxide layer and growth of fine needle-type Cr_2O_3 grains were observed as displayed in Fig. 16 (a). The bumps or protrusions are indications of delamination or formation of bubbles within the Cr_2O_3 layer (Fig. 16 (b)). At the hottest region, a fairly uniform and thick ZrO_2 layer grew beneath the surface Cr_2O_3 layer (Fig. 16 (c)). The Cr coating has almost completely disappeared, apart from a few spots where metallic Cr particles were embedded in the Cr_2O_3 oxide layer, as revealed in the zoomed image in Fig. 16 (c). In addition, the Zircaloy-4 substrate showed some signs of melting in the inner side of the tube, which could be attributed to oxidation (oxygen) driven inward diffusion of Cr into the inner region of the cladding as reported previously [8,9]. The evolution of the cross section microstructure from the cold region (upper) to the hot region (middle) is shown in Fig. 16 (d). The maximum temperature measured by the TC_u was ~1025°C. The Cr coating was protective at the upper region without obvious oxidation of the substrate. However, some discontinuity of the Cr coating layer was seen, probably owing to local spallation of the thin coating layer during metallographic treatment. As the region shift to hot areas, oxidation of the substrate accompanied by significant inward diffusion of the Cr coating into the substrate were revealed. Finally, a uniform ZrO_2 layer formed beneath the Cr_2O_3 layer on the surface.

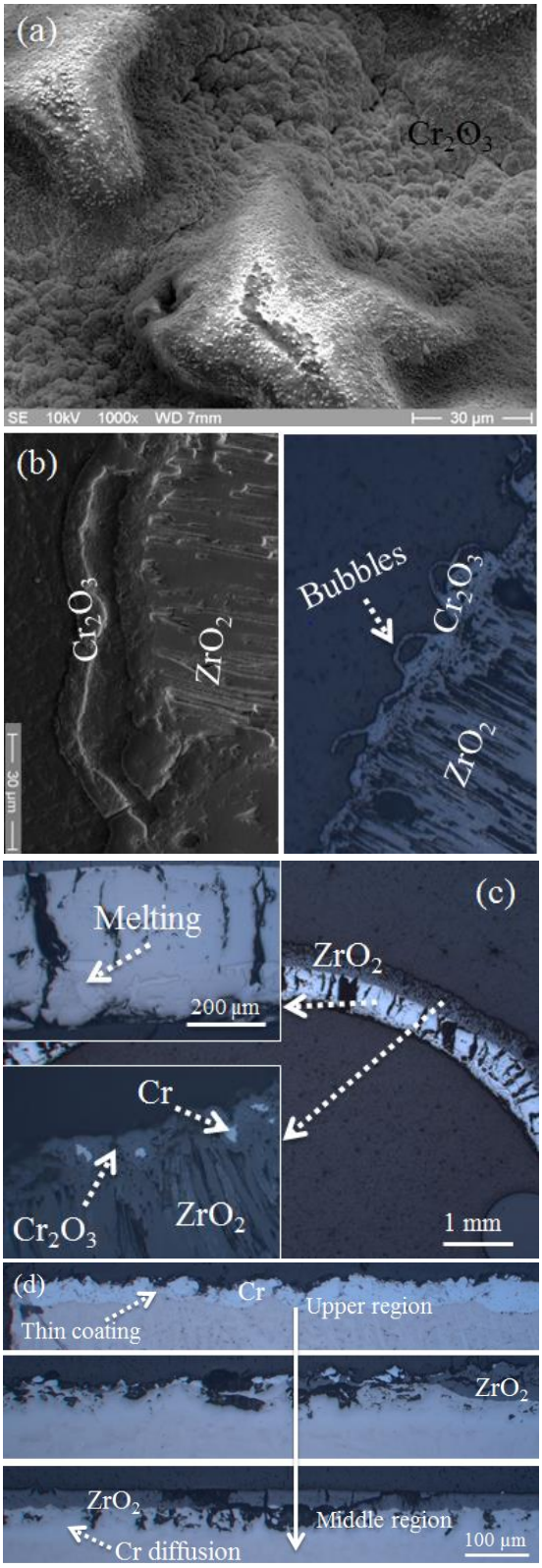

Fig. 16. Surface and cross section microstructures of the Cr coated tube after the transient test. (a) Surface structure at ~53 mm location, cross section of (b) and (c) at ~53 mm location and (d) from upper to middle region.

IV. DISCUSSION

Bending phenomenon of the coated cladding was only seen during isothermal oxidation at 1100°C, both without and with pre-oxidation from 800°C in steam. The underlying mechanisms making the bending are not completely understood yet. The interpretations seem to be connected with the residual stress state and high-temperature creep behavior of the coated cladding. In cold spray process, feedstock powders are propelled to supersonic velocities and are sprayed on to the surface of a substrate to form a dense and adherent coating via high-strain-rate plastic deformation of particles and an associated adiabatic shear mechanism [13]. The mechanical impact of the high-velocity spraying particles typically leaves a high-level of residual stress and stress concentration (inhomogeneity) within the coating/substrate system. In addition, severe plastic deformation of the bulk surface also happens, strengthening and hardening the cladding tube surface and slightly reducing its ductility [14]. Since one end of the tube was not coated and temperature gradient existed along the tube axis (contributing to additional thermal stress), deformation (or creep) of the cladding tube will be trigged to relieve the residual stress at certain temperatures especially at the coated end. Weak degree of bending was measured before the steam oxidation at 1100°C, and most of the bending took place just after the steam was introduced. The tensile side of the bending tube resulted in the cracking of the coating layer, which contributes to the loss of protective effect and fast oxidation of the Zircaloy-4 substrate. Thus, the strength of the two sides of the cladding tube was quite different after oxidation, which may have accelerated the bending of the cladding. At higher temperatures, the cladding is much softer and the residual stress probably could be quickly relieved. Therefore, no obvious bending of the cladding tube was observed. The bending leads to local failure of the coating and can exacerbate the degradation of the cladding compared to the uncoated one owing to heavily non-uniform oxidation at the maximum strain locations. To fully elucidate the underlying mechanisms for the occurrence of the bending phenomenon at such temperature, more investigations are required.

The coated cladding tube performed well with considerably reduced oxidation rate and hydrogen production during isothermal oxidation at 1200°C and good thermal shock resistance with subsequent quenching, except some delamination was seen at the interfaces. The reasons for the delamination seems to be related with the high roughness of the coating surface and coating/substrate interface (may leading to stress concentration) typical for cold spraying coatings.

The melting of the cladding tube during the oxidation test at 1300°C was unexpected. The detachment of the thermocouple with the cladding finally contributed to failure of temperature control and much higher temperature of the cladding was anticipated. Large liquid drops were seen after the test and the cladding degraded severely.

Transient test up to 1500°C indicates that oxygen drives the Cr diffusing inwardly (owing to low solubility of Cr in ZrO_2 [15]) and formation of liquid phase in the inner side of the cladding tube. Formation of liquid drops accompanied by its continuous displacement and movement and partial reducing of the chromia layer can disturb the continuity of the surface oxide layer. The coating layer lost the protective capability quickly (via oxidation and inward diffusion) and a much faster oxidation rate was detected caused by oxidation of the fresh Zircaloy-4 substrate. Oxidation-induced consumption of the metallic Cr coating layer reduces the volume of the liquid phase during the transient test compared to the failed isothermal test at 1300°C. Thus, an optimized coating thickness should be pursued to provide sufficiently enhanced accident tolerance as well as to avoid substantial formation of liquid phase during severe accidents. Another option can be deposition of an interlayer as a robust barrier. Formation of bubbles within the Cr_2O_3 layer seems due to the enhanced volatilization rate of Cr_2O_3 via formation of hydroxides at elevated temperatures in steam [16]. Both tests have proved that the protective capability of the Cr coating was highly challenged and worse performances of the coated cladding may occur once the temperature exceeds the Cr-Zr eutectic temperature.

V. CONCLUSIONS

Steam oxidation with subsequent water quench of cold spraying Cr coated Zircaloy-4 tube in this study confirmed the significantly improved oxidation resistance and excellent adherence of the Cr coating layer, which can provide considerably enhanced accident tolerance up to the Cr-Zr eutectic reaction temperature (~1330°C).

However, undesirable substantial bending of the coated cladding occurred at 1100°C. Loss of protective effect and fast oxidation of the Zircaloy-4 substrate took place at the tensile (convex) side of the bending owing to coating layer cracking and spallation. A likely explanation is that the high level of residual stress associated with stress concentration (inhomogeneity) within the coating/substrate system and severe plastic deformation of the substrate bulk surface typical for cold spraying process resulted in creep induced bending of the cladding at such temperature. At higher temperatures, the residual

stress can be quickly relieved and the cladding becomes much softer, thus no bending occurs.

Above the Cr-Zr eutectic temperature, fast interdiffusion and formation of liquid phase led to quick degradation of the coated cladding with even higher oxidation kinetics relative to uncoated one. Oxygen drives the Cr diffusing inwardly leading to formation of liquid phase in the inner side of the cladding tube. An optimized coating thickness thus should be pursued to provide sufficiently enhanced accident tolerance as well as to avoid substantial formation of liquid phase during severe accidents.

More investigations are required to fully elucidate the underlying mechanisms for the occurrence of the bending phenomenon at intermediate temperature (~1100°C) and the failure behaviors at elevated temperatures (>1330°C) of the clod spraying Cr coated fuel claddings. Furthermore, comparison with Cr coatings produced by other techniques like PVD on modern Zircaloy alloys such as Zirlo or M5 is of great interest.

ACKNOWLEDGMENTS

This work was sponsored by the HGF program NUSAFE at Karlsruhe Institute of Technology. The authors thank U. Stegmaier and N. Neuraij for conducting the experiments and support during the post-test examinations.

REFERENCES

1. S.J. Zinkle, K.A. Terrani, J.C. Gehin, L.J. Ott, L.L. Snead, Accident tolerant fuels for LWRs: A perspective, J. Nucl. Mater. 448 (2014) 374–379.
2. K.A. Terrani, Accident tolerant fuel cladding development: Promise, status, and challenges, J. Nucl. Mater. 501 (2018) 13–30.
3. C. Tang, M. Stueber, H.J. Seifert, M. Steinbrueck, Protective coatings on zirconium-based alloys as accident-tolerant fuel (ATF) claddings, Corros. Rev. 35 (2017) 141–166.
4. J.C. Brachet, M. Le Saux, V. Lezaud-Chaillioux, M. Dumerval, Q. Houmaire, F. Lomello, et al., Behavior under LOCA conditions of Enhanced Accident Tolerant Chromium Coated Zircaloy-4 Claddings, in: TopFuel, 2016: pp. 1173–1178.
5. A.S. Kuprin, V.A. Belous, V.N. Voyevodin, R.L. Vasilenko, V.D. Ovcharenko, G.D. Tolstolutskaya, et al., Irradiation resistance of vacuum arc chromium coatings for zirconium alloy fuel claddings, J. Nucl. Mater. 510 (2018) 163–167.
6. J.-C. Brachet, I. Idarraga-Trujillo, M. Le Flem, M. Le Saux, V. Vandenberghe, S. Urvoy, et al., Early studies on Cr-Coated Zircaloy-4 as enhanced accident tolerant nuclear fuel claddings for light water reactors, J. Nucl. Mater. 517 (2019) 268–285.
7. B. Maier, H. Yeom, G. Johnson, T. Dabney, J. Walters, P. Xu, et al., Development of cold spray chromium coatings for improved accident tolerant zirconium-alloy cladding, J. Nucl. Mater. 519 (2019) 247–254.
8. J. Krejci, M. Sevecek, J. KABÁTOVÁ, F. MANOCH, J. KOČÍ, L. CVRČEK, et al., Experimental behavior of chromium-based coatings, in: TopFuel, 2018: pp. 1–14.
9. J. Brachet, T. Guilbert, M. Le Saux, J. Rousselot, G. Nony, C. Toffolon-Masclet, et al., Behavior of Cr-coated m5 claddings during and after high temperature steam oxidation from 800 °C up to 1500 °C, in: TopFuel, 2018: pp. 1–11.
10. M. Ševeček, A. Gurgen, A. Seshadri, Y. Che, M. Wagih, B. Phillips, et al., Development of Cr cold spray–coated fuel cladding with enhanced accident tolerance, Nucl. Eng. Technol. 50 (2018) 229–236.
11. M. Steinbrück, J. Birchley, A. V. Boldyrev, A. V. Goryachev, M. Grosse, T.J. Haste, et al., High-temperature oxidation and quench behaviour of Zircaloy-4 and E110 cladding alloys, Prog. Nucl. Energy. 52 (2010) 19–36.
12. H. Baker, H. Okamoto, ASM Handbook. Vol. 3. Alloy Phase Diagrams, 1992.
13. H. Assadi, H. Kreye, F. Gärtner, T. Klassen, Cold spraying – A materials perspective, Acta Mater. 116 (2016) 382–407.
14. D.J. Park, H.G. Kim, Y. Il Jung, J.H. Park, J.H. Yang, Y.H. Koo, Microstructure and mechanical behavior of Zr substrates coated with FeCrAl and Mo by cold-spraying, J. Nucl. Mater. 504 (2018) 261–266.
15. H.P. Beck, C. Kaliba, On the solubility of Fe, Cr and Nb in ZrO_2 and its effect on thermal dilatation and polymorphic transition, Mater. Res. Bull. 25 (1990) 1161–1168.
16. P.J. Meschter, E.J. Opila, N.S. Jacobson, Water Vapor–Mediated Volatilization of High-Temperature Materials, Annu. Rev. Mater. Res. 43 (2013) 559–588.